Radiation Products in Processed Ices Relevant to

Edgeworth-Kuiper-Belt Objects

M. H. Moore

NASA/Goddard Space Flight Center
Greenbelt, MD 20771
Marla.H.Moore@nasa.gov

R. L. Hudson

Eckerd College
St. Petersburg, FL 33733
hudsonrl@eckerd.edu

R. F. Ferrante

US Naval Academy
Annapolis, MD 21402
ferrante@usna.edu

Send Correspondence to:

Marla H. Moore
Code 691, Astrochemistry Branch
NASA/Goddard Space Flight Center
Greenbelt, MD 20771
301-286-9031 (p)
301-286-0440 (f)

Abstract

Near the inner edge of the Edgeworth-Kuiper Belt (EKB) are Pluto and Charon, which are known to have N_2- and H_2O-dominated surface ices, respectively. Such non-polar and polar ices, and perhaps mixtures of them, also may be present on other trans-Neptunian objects. Pluto, Charon, and all EKB objects reside in a weak, but constant UV-photon and energetic ion radiation environment that drives chemical reactions in their surface ices. Effects of photon and ion processing include changes in ice composition, volatility, spectra, and albedo, and these have been studied in a number of laboratories. This paper focuses on ice processing by ion irradiation and is aimed at understanding the volatiles, ions, and residues that may exist on outer solar system objects. We summarize radiation chemical products of N_2-rich and H_2O-rich ices containing CO or CH_4, including possible volatiles such as alcohols, acids, and bases. Less-volatile products that could accumulate on EKB objects are observed to form in the laboratory from acid-base reactions, reactions promoted by warming, or reactions due to radiation processing of a relatively pure ice (e.g. $CO \rightarrow C_3O_2$). New IR spectra are reported for the 1 - 5 μm region, along with band strengths for the stronger features of carbon suboxide, carbonic acid, the ammonium and cyanate ions, polyoxymethylene, and ethylene glycol. These six materials are possible contributors to EKB surfaces, and will be of interest to observers and future missions.

Key Words:

Comets

EKBOs

Ice

Infrared Spectra

Radiation Chemistry

1. Introduction

A summary of this paper was presented at the First Decadal Review of the Edgeworth-Kuiper-Belt: Towards New Frontiers workshop in Antofagasta, Chile. The workshop's focus was to review scientific knowledge of the Edgeworth-Kuiper Belt (EKB); participants included observers, theorists, and experimentalists. The workshop made clear that the EKB, a reservoir from which short period comets are recruited, is on the verge of further characterization by new surveys; these are expected to dramatically increase the number of known objects in this region. In addition, future missions will target several of these cold icy bodies for a more in-depth examination. Laboratory research directed towards understanding the composition, chemistry, and color of Kuiper Belt objects (KBOs) were workshop topics.

A major focus of our own laboratory work is the low-temperature radiation chemistry of ices and the identification of likely products for remote detection. This paper summarizes some of our laboratory results on products identified in processed H_2O- and N_2-rich ice mixtures relevant to KBOs. New spectra in the 1 - 5 μm region for several of the least volatile radiation products are presented along with intrinsic band strengths of the more intense features.

Table I lists ices, organics, and complex materials identified on objects located near the edge of the solar system. These identifications are described in several recent papers. Cruikshank *et al.* (1998), and Luu *et al.* (2000), and references therein, reported the detection of H_2O-ice on various Centaurs. N_2-rich ice containing small amounts of methane (CH_4) and carbon monoxide (CO) was identified on the surfaces of Pluto and Triton (Cruikshank *et al.*, 1993; Owen *et al.*, 1993). Relative abundances of N_2:CH_4:CO

on Triton of 100:0.1:0.05 (Quirico *et al.*, 1999) and 100:0.5:0.25 on Pluto (Doute *et al.*, 1999) were determined by detailed comparisons of observations and laboratory spectra. Ice features dominated by H_2O, and possibly containing NH_3 absorptions, were detected on Charon (Brown and Calvin, 2000; Buie and Grundy, 2000; Dumas *et al.*, 2001). Noll *et al.*, 2000 and Brown *et al.*, 2000, discuss features detected in spectra of several KBOs. For comets, coma molecules arise from the sublimation of H_2O-dominated ices. (Ehrenfreund and Charnley, 2000, give an inventory of these volatiles.) Although observing a comet's nucleus is more difficult than observing its coma, broad absorption features at 1.5 and 2.05 μm in Hale-Bopp spectra are thought to arise from water ice on the nucleus (Davies *et al.*, 1997). Another cometary nuclear absorption, at 2.39 μm, was measured during the DS-1 encounter with Borrelly and is consistent with C-H compounds (Soderblom *et al.*, 2002).

Compositional differences among the icy objects at the edge of the solar system can be understood, in part, by variations in temperature, which affect vapor pressures, and masses, which affect escape velocities. Surface temperatures of Triton, Pluto, and Charon are in the 30 - 40 K range, and temperatures of KBOs and comets beyond 40 AU are under 30 K. Although Pluto and Triton are cold enough and massive enough to retain N_2, CH_4, and CO ices, similar volatiles detected in comets must have been trapped in H_2O ice. Centaurs are the presumed transition objects between KBOs and short-period comets, and are in unstable orbits in the giant planet region. Their surfaces are warmer than Triton's and probably depleted of N_2, CO, and CH_4, but they could still preserve these molecules if trapped in an H_2O matrix in cooler inner layers.

A common feature among all these objects is their exposure to UV photons and cosmic ray particles (mostly H^+, He^+, and O^+), which slowly modify the chemistry of surface ices. Estimates of relevant incident fluxes are given in Table I. Johnson (1989) has discussed the results of these processes. UV photons absorbed in the atmospheres of Triton and Pluto can form products that precipitate onto their icy surfaces, but on surfaces without atmospheres the observed contribution of UV exposure is small. The reason for this is that the UV penetration depth is only ~ 0.15 μm, compared to the ~ 50-μm thickness of ice sampled by IR observations. Turning to particle radiation, Table I gives an approximate energy flux for 1 MeV cosmic rays (CR). From such an estimate, Johnson (1989) calculated a dose of 160 eV $molec^{-1}$ deposited in the top 100 g cm^{-2} of material on Pluto (i.e., 1 meter for a density of 1 g cm^{-3}), and he estimated that this dose could alter 60% of the condensed species. In addition, data from the Voyager and Pioneer spacecraft near the edge of the solar system show a significant intensity for an anomalous cosmic ray (ACR) component of H^+ and heavier ions which cause additional processing of surface layers (Cooper *et al.*, 1998, 2003). For example, at 40 AU the ACR 1MeV H^+ flux is an order of magnitude greater than the CR 1 MeV H^+ flux (see Cooper *et al*., 2003). Focusing on the μm-to-cm thick layers of ices that are accessible to remote sensing observations, the accumulation of altered species from CR and ACR radiation over many orbits can produce an appreciable mantle of radiation-processed material on time scales comparable or even shorter than disruptive processes such as collisions (Cooper *et al*., 2003). Therefore, understanding the composition and possible radiation chemical influences on ices is important for unraveling the connections between short

and long period comets, KBOs, and Centaurs, and the roles of N_2- and H_2O-rich ice chemistries.

The influence of MeV protons on molecules is known in general terms. Each incident H^+ (~ 1 MeV) creates a trail of thousands of ionizations and excitations along its path through an ice, as its energy is slowly degraded. Some of the ionizations will produce secondary electrons, which, in turn, will create separate tracks of yet more ionizations and excitations that lead to further chemical changes. For H_2O ice, the total range traveled by a 1 MeV proton is near 23 μm, but higher-energy protons have greater penetration depths and can process the top 100 g cm^{-2} of icy surface material. In addition, secondary nuclear and electromagnetic showers from CR or ACR can penetrate tens of meters.

Although the molecules in Table I are relatively simple, quantitative predictions of their responses to radiation are difficult. For this reason, laboratory experiments continue to provide the ground truth that documents radiation-induced chemical changes. Here we first summarize our laboratory IR studies, from 2.5 - 25 μm, of some irradiated ices (H_2O and N_2 ices containing CO and CH_4) relevant to the surfaces of outer solar system objects. Results from these experiments show which ions and molecules are detectable at different temperatures. The bulk of this paper then follows, and focuses on new IR spectra, from 1 - 5 μm, of several relatively involatile species that may be KBO surface materials. Intrinsic band strengths are given for many of the stronger IR features.

2. Experimental Methods

Details of our experimental set-up, ice preparation, IR spectral measurements, cryostat, and proton beam source have been published (Moore and Hudson, 2000; Moore and Hudson, 1998; Hudson and Moore, 1995). In summary, ice samples were formed by condensation of gas-phase mixtures onto a pre-cooled aluminum mirror at 10 - 20 K. Two spectrometers allowed measurements from 1 - 5 μm (Brucker spectrometer) and from 2.5 - 25 μm (Mattson spectrometer). Figure 1 is a schematic that represents the design of both set-ups. Most ice films examined between 1 and 5 μm were tens of microns thick, as determined by a laser interference fringe system. Spectra were measured as a function of temperature (12 - 300 K) in some experiments.

IR spectra were recorded before and after exposure of ices to a 0.8 MeV proton beam from a Van de Graaff accelerator. The use of proton irradiation to simulate cosmic-ray bombardment has been discussed in other papers (e.g., Hudson and Moore, 2001; Moore *et al.*, 1983). Three ice experiments (NH_3 + HCl, NH_3 + HNCO, and NH_3 + H_2CO) involved no irradiation because the desired products formed during warming. Several band strengths (either A values or cross sections) are reported for the first time. Some of these were calculated by scaling previously-published values, based on the relative areas of our spectral bands compared to the area of a previously-measured band. For ethylene glycol, $A((CH_2OH)_2)$ was measured using an injection technique to form different thicknesses of H_2O + $(CH_2OH)_2$, following a procedure described in Moore and Hudson (2000).

Carbon suboxide, C_3O_2, was generated by a method described by Gerakines and Moore (2001). HNCO was synthesized by the reaction of NaOCN powder (Aldrich

Chemical, 96%) with HCl gas (Aldrich Chemical 99+%), and purified by distillation from an ethanol/liquid nitrogen slush bath. Formaldehyde (H_2CO) was the gas released during the warming of paraformaldehyde. Ethylene glycol, $(CH_2OH)_2$, was from Fisher Scientific, certified. Other reagents used were the same purity as those referenced by Cottin *et al.* (2003).

3. Radiation Products in H_2O and N_2 Ices Containing CO and CH_4

3.1 H_2O-rich ices

A summary of products from processed H_2O-rich ices, containing either CO or CH_4, is included here for completeness. These mixtures are relevant to both comets and KBOs. Hudson and Moore (1999) examined H_2O + CO ices to follow the low-temperature, solid-phase sequence CO $\rightarrow$ H_2CO $\rightarrow$ CH_3OH. We showed that H_2CO and CH_3OH formed with greater abundances than reported by other condensed-phase processes (UV-photolysis and discharge experiments). Radiation-processed ices had a ratio $CH_3OH/H_2CO \sim 1.7$, which is near the value of 2 observed for comets and interstellar ices. Spectral studies of the radiation chemistry of H_2O + CH_4 ices (Moore and Hudson, 1998) were motivated by the discovery of abundant C_2H_6 in comet C/1996 B2 Hyakutake by Mumma *et al.* (1996). The role of CH_4 for C_2H_6 formation in irradiated icy mixtures was examined. A summary of the radiation products we identified is given in Table II, which also lists species whose spectral signatures were still present as ices were warmed to ~100 K.

3.2 N_2-rich ices

We also have recently published IR (2.5 - 25 μm) studies of proton irradiated N_2-dominated ices (Moore and Hudson, 2003). Mixtures of N_2 + CH_4, N_2 + CO, and N_2 + CH_4 + CO are relevant to ices identified on Pluto and Triton. Products formed during irradiation at 10 - 20 K were identified as HCN, HNC, NH_3, HN_3, OCN^-, and CH_2N_2 (diazomethane). The evolution and stability of these products were followed during warming to ~ 35 K, where OCN^-, CN^-, N_3^-, and NH_4^+ were identified. We expect that similar species exist on the surfaces of Triton, Pluto, and perhaps KBOs. Even with further warming, all of these ions were detectable at 100 K. These results are summarized in Table II.

4. Spectra (1 - 5 μm) and Band Strengths of Products Observed Above ~ 100 K

In this section we show 1 - 5 μm spectra of some of the more stable radiation products and give peak positions for many of the weaker absorption bands. These weaker features can include both overtone and combination bands, which we will refer to as overtones in the following sections. Selection of these products is based on results shown in Table II. Four identified products present at 100 K are: carbon suboxide (C_3O_2), carbonic acid (H_2CO_3), and the ammonium (NH_4^+) and cyanate (OCN^-) ions. Also included for study are polyoxymethylene (POM or $(H_2CO)_n$) and ethylene glycol (($CH_2OH)_2$), because these are stable radiation end-products of molecules observed in irradiated H_2O-rich ices (H_2CO and CH_3OH, respectively).

4.1 Carbon suboxide (C_3O_2)

Irradiation of pure CO ice at 20 K forms CO_2, C_2O, and C_3O_2, the latter being the least volatile of the three. Figure 2 shows the 1 - 5 μm spectrum of C_3O_2 at 10 K compared to the spectrum of pure unirradiated CO at 10 K (shown truncated at the bottom of the figure). The C_3O_2 spectrum from 1 - 4 μm was measured using a 50-μm thick ice, compared to a 5-μm thick ice for the strong 4.55 μm feature. An expansion shows weak features at 2.19, 2.29, and 2.34 μm after removal of the underlying channel fringe pattern. A recent study by Gerakines and Moore (2001) discussed the formation and stability of carbon suboxide in proton-irradiated and UV-photolyzed ices. That work included the C_3O_2 IR spectrum from 2.0 - 25 μm, and the identification and band strengths of the strongest absorptions. The 1 - 5 μm spectrum reported in the present paper overlaps significantly with the spectral region covered by Gerakines and Moore (2001), but because thicker samples were used in our current experiments we also obtained positions of weaker features (see Table III). Band strengths were calculated by scaling the published A-values for the 3.29 μm feature by the ratio of the band areas, e.g. $A(3.63 \text{ μm}) = A(3.29 \text{ μm}) \times (\text{band area, } 3.63 \text{ μm}) \times (\text{band area, } 3.29 \text{ μm})^{-1}$.

4.2 Carbonic acid (H_2CO_3)

Irradiation of the two-component ice $H_2O + CO_2$ at 10 - 20 K forms CO, H_2O_2, O_3, and H_2CO_3, the last being the least volatile species. Figure 3 compares the 1 - 5 μm spectrum of pure H_2CO_3 at 250 K with the truncated spectrum of unirradiated $H_2O + CO_2$ (10:1) at ~ 20 K. Previous IR (2.5 - 25 μm) studies of H_2CO_3 formation, stability, and A-values can be found in Moore and Khanna (1991), DelloRusso *et al.* (1993), and

Gerakines *et al.* (2001). The IR spectrum of H_2CO_3 also has been identified in pure CO_2

ices implanted with H^+ (Brucato *et al.*, 1997). No new H_2CO_3 features were found in the

1 - 2.5 µm region within the limits of detection. The *A*-value for the 3.82 µm band at 250

K was calculated from the 18 K value published in Gerakines *et al.* (2000) in a manner

similar to that described above: A(3.82 µm, 250 K) = A (3.81 µm, 18 K) × (band area

3.82 µm, 250 K) × (band area 3.81 µm, 18 K)$^{-1}$.

4.3 Ammonium chloride (NH_4Cl)

Figure 4 shows the 1 - 5 µm spectrum of NH_4Cl, made by simultaneously

condensing (from separate deposit tubes) NH_3 and HCl at ~ 20 K, and then warming to

250 K. The spectrum of pure NH_3 at 120 K is given for comparison, while HCl's only

absorption in this region is at 3.6 µm (arrow). Strong, well-defined peaks at 3.20 and

3.28 µm, and a less-defined one at 3.52 µm, are due to the ammonium ion (NH_4^+). An

expansion in the 2.0 - 2.3 µm region shows weaker NH_4^+ bands at 2.21 and 2.24 µm, and

is compared to the same region for pure NH_3 at 120 K. Previous IR studies involving

NH_4^+ have focused on the 6.96 µm feature (e.g. Grim *et al.*, 1989; Demyk *et al.*, 1998;

Keane 1997; Khanna, 2003, private communication). *A*-values in Table II were

calculated for bands in the 1 - 5 µm region by scaling the average reported values for the

6.96 µm band (30×10^{-18} cm molec^{-1}) with the ratio of the band areas, as described

earlier.

4.4 Ammonium cyanate (NH_4OCN)

The IR spectrum of NH_4OCN from 1 - 5 μm at 250 K, compared to the truncated spectrum of pure HNCO at 10 K, is shown in Figure 5. Acid-base reactions were promoted on warming NH_3 + HNCO (reactants condensed simultaneously from separate deposit tubes), and the formation of NH_4^+ and OCN^- occurred. The ammonium ion features at 3.16, 3.29, and 3.51 μm are broader than those of NH_4Cl shown in Figure 4, but show the same relative band areas. Previous IR (2.5 - 25 μm) studies of OCN^- formation, its stability, and its A-value can be found in Grim and Greenberg (1987), d'Hendecourt and Allamandola (1986), and Hudson et $al.$ (2001). In our 1 - 5 μm spectrum, the large OCN^- band at 4.61 μm was the only anion absorption feature found within our limits of detection. Weaker NH_4^+ overtone bands were not observed since the sample's thickness was an order of magnitude less than that for Figure 4.

4.5 Polyoxymethylene (($H_2CO)_n$)

Schutte et $al.$ (1993) showed that reactions during warming an ice mixture of H_2CO + NH_3 (where the H_2CO/NH_3 ratio is 50) produces polyoxymethylene (POM or ($H_2CO)_n$). We used this technique to produce the 1 - 5 μm spectrum of POM at 200 K shown in Figure 6. For comparison, the spectrum of pure H_2CO at 20 K is at the bottom of Figure 6 (the NH_3 spectrum is in Figure 4). An alternate method for making POM (without warming in the presence of NH_3) is the irradiation of pure H_2CO ice at 20 K. On irradiation, pure H_2CO ice forms CO, CO_2, HCO, and POM, the last being the least volatile species. The spectrum of POM from irradiated H_2CO is not presented in this paper. Our IR spectrum of POM has bands at 3.35, 3.42, and 3.58 μm which agree with

13

those reported by Schutte *et al.* (1993), and which are attributed to stretching vibrations. The 2.94 μm feature we see is most likely due to O-H bonded species from H_2O contamination. A distinct, sharp absorption of POM at 2.24 μm is shown in the expanded region of Figure 6. The cross section of this band is given in Table III, and was derived by scaling the 2.24 μm area with the area of the 3.58 μm band and using the cross section for the 3.58 μm band, 8.5×10^{-21} cm^2 (C-atom)$^{-1}$, of Schutte *et al.* (1993). We cannot readily compare POM band intensities with those of other species because band strengths for a polymer are described only by a cross section value if the polymer's chain length is unknown, as it is here.

4.6 Ethylene glycol $(CH_2OH)_2$

Irradiation of pure CH_3OH ice at 10 - 20 K formed a variety of reaction products, such as CH_4, CO, CO_2, H_2CO, H_2O, HCO, $HCOO^-$, and $(CH_2OH)_2$, with the last being the least volatile (Hudson and Moore, 2000). The 1 - 5 μm spectrum of $(CH_2OH)_2$ at 10 K is shown in Figure 7, and is compared to the spectrum of pure unirradiated CH_3OH at 10 K (shown truncated at the bottom of the figure). The positions of bands within the 1 - 5 μm region, and several *A*-values, are listed in Table III. Weak bands at 2.10, 2.29, and 2.49 μm are shown on an expanded scale in Figure 7, and compared to CH_3OH absorptions. Previous IR studies from 2.5 - 25 μm of irradiated CH_3OH, describing new products and band profile changes, include Moore *et al.* (1996), Hudson and Moore (2000), and Palumbo *et al.* (1999).

14

5. Discussion

To understand the chemistry of comets, KBOs, Triton, and Pluto it is necessary to understand the composition and reactivity of their icy surfaces. H_2O-rich ices containing CH_4 or CO are relevant for this task. Irradiation of $H_2O + CH_4$ and $H_2O + CO$ at 10 - 20 K shows that the products with the largest abundances are CH_3OH and CO_2, respectively. Further processing of CH_3OH, either in the presence or absence of H_2O, produces the less-volatile ethylene glycol (Hudson and Moore, 2000), a molecule we have investigated in this paper. Similarly, further irradiation of CO_2 in H_2O gives H_2CO_3 (Gerakines *et al.*, 2000), which we also have included in this paper. By examining the 1 - 5 μm spectra of both $(CH_2OH)_2$ and H_2CO_3, and comparing intrinsic band strengths, we find that H_2CO_3 has the larger *A* value. In fact, on a surface composed of equal abundances of H_2CO_3, C_2O_3, NH_4^+, OCN^-, and $(CH_2OH)_2$, it is H_2CO_3 that would have the most intense IR band (Table III).

Carbonic acid and methanol are not the only products found in irradiated $H_2O + CO$ and $H_2O + CH_4$ ices. Less abundant products are formed and can remain trapped in the H_2O, even on warming to 100 K. Such products include ethanol (C_2H_5OH), formic acid (HCOOH), formaldehyde (H_2CO), and ethane (C_2H_6).

Because as much as 19% of the total carbon in $H_2O + CO$ ice can be converted to H_2CO by irradiation (Hudson and Moore, 1999), we also have examined the radiation processing of H_2CO, which leads to a less-volatile molecule, POM. It is also possible to form this polymer through thermally-promoted reactions of H_2CO in the presence of NH_3. Since POM has been suggested as a candidate to explain mass spectra taken by Giotto near comet Halley (Huebner, 1987), the study of this polymer is important.

Irradiated N_2-rich ices containing CO and CH_4 are relevant for understanding the surfaces of Triton and Pluto. The radiation products expected to form and survive on these surfaces are anions (OCN^-, CN^-, and N_3^-) associated with the cation, NH_4^+. For this reason we investigated the 1 - 5 μm spectra of both NH_4Cl and NH_4OCN. The 4.6-μm bands was the only detected OCN^- absorption. It is a good candidate for future observations because it is moderately intense and lies in a region not obscured by H_2O bands. The strongest NH_4^+ bands lie within the intense 3.1-μm feature of H_2O. The weak NH_4^+ overtones in the 2.0 - 2.2 μm region become good candidates for new observations, although the 2.2-μm absorption is close to one of the weak NH_3 overtones, as seen in Figure 4.

The possibility of terrains on Pluto and Triton with varying concentrations of CO, CH_4, and N_2 led us to also investigate the conversion of pure CO into C_3O_2 during irradiation. Brownish-red in color, C_3O_2 has been proposed as a possible surface colorant for cometary nuclei (Huntress *et al.*, 1991). In the 1 - 5 μm region it has a very strong feature at 4.55 μm, along with many weaker overtone bands.

Each of the six species listed in Table III can be formed in irradiated ices. In the absence of evidence for thermal processing, all six could be markers for radiation processing. POM, NH_4^+, and OCN^- also can form during thermal processing of ices containing the reactants for acid-base reactions or NH_3-catalyzed reactions. Since there is no known reasonable thermal, catalytic, or acid-base processing that could explain the presence of C_3O_2, H_2CO_3, and $(CH_2OH)_2$ in outer solar system ices, these three molecules are reliable markers for radiation-induced chemistry.

Future laboratory work will include careful studies of band profiles at different temperatures for these six ions and molecules, along with other possible surface species. Such spectra are important for determining if any characteristic profiles exist that can be used as temperature markers (e.g. the 1.65 μm band of crystalline water ice). In addition, more work needs to be done before some of these species can be distinguished from more abundant molecules. For example, it may be difficult to discriminate between CH_3OH and $(CH_2OH)_2$. Similarly, the difference between NH_4^+ and NH_3 may require more work, especially if NH_3-hydrates are considered.

Acknowledgements

References

Brown, M. E. and Calvin, W. M.: 2000, *Science* **287**, 107-109

Brown, M. E., Blake, G. A., Kessler, J. E.: 2000, *ApJ* **543**, L163-L165

Brucato, J. R., Palumbo, M. E., and Strazzulla, G.: 1997, *Icarus* **125**, 135-144

Buie, M. W. and Grundy, W. M.: 2000, *Icarus* **148**, 324-239

Cooper, J. F. Christian, E. R., and Johnson, R. E.: 1998, *Adv. Space Res.* **21**, 1611-1614

Cooper, J. F., Christian, E. R., and Johnson, R. E.: 2003, *This Journal*

Cottin, H., Moore, M. H., and Benilan, Y.: 2003, *ApJ*, in press

Cruikshank, D. P., Roush, T. L., Owen, T. C., Geballe, T. R., de Bergh, C., Schmitt, B. Geballe, T. R., Barthlomew, M. J.: 1993, *Science* **261**, 742-745

Cruikshank, D. P., Roush, T. L., Bartholomew, M. J., Geballe, T. R., Pendleton, Y. J., White, S. M., Bell III, J. F., Davies, J. K., Owen, T. C., de Bergh, C., Tholen, D. J., Bernstein, M. P., Brown, R. H.: 1998, *Icarus* **135**, 389-407

Davies, J. K., Roush, T. L., Cruikshank, D. P., Bartholomew, M. J., Geballe, T. R., Owen, T. de Bergh, C.: 1997, *Icarus* **127**, 238-245

DelloRusso N., Khanna, R. K., Moore M. H.: 1993, *J. Geophys. Res.* **98**, 5505-5510

Demyk, K. Dartois, E., d'Hendecourt, L., Jourdain de Muizon, M., Heras, A. M., Breitfellner, M.: 1998, *Astron. Astrophys.* **339**, 553-560

d'Hendecourt, L. B. and Allamandola, L. J.: 1986, *Astron. Astrophys. Supp. Ser.* **64**, 453-467

Doute, S., B. Schmitt, E. Quirico, T. C. Owen, D. P. Cruikshank, C. de Bergh, T. R. Geballe, and T. L. Roush: 1999, *Icarus* **142**, 421-444

Dumas, C., Terrile, R. J., Brown, R. H., Schneider, G., Smith, B. A.: 2001, *ApJ* **121**, 1163-1170

Ehrenfreund, P. and Charnley, S. B: 2000, *Ann. Rev. Astron. Astrophys* **38**, 427-483

Gerakines, P. A., Moore, M. H., and Hudson, R. L.: 2000, *Astron. Astrophys.* **357**, 793-800

Gerakines, P. A. and Moore, M. H.: 2001, *Icarus* **154**, 372-280

Grim, R. J. A., Greenberg, J. M., deGroot, M. S., Baas, F., Schutte, W. A., Schmitt, B.: 1989, *Astron. Astrophys. Suppl. Ser.* **78**, 161-186

Grim, R. J. A. and Greenberg, J. M.: 1987, *ApJ* **321**, L91-L96

Hudson, R. L. and Moore, M. H.: 1995, *Rad. Phys. and Chem.* **45**, 779-789

Hudson, R. L. and Moore, M. H.: 1999, *Icarus* **140**, 451-461

Hudson, R. L. and Moore, M. H.: 2000, *Icarus* **145**, 661-663

Hudson, R. L., and Moore, M. H.: 2001, *J. Geophys. Res. - Planets* **106**, 33275-33284

Hudson, R. L., Moore, M. H., and Gerakines, P. A.: 2001, *ApJ.* **550**, 1140-1150

Huebner, W. F.: 1987, *Science* **237**, 628-630

Huntress, W. T. Jr., Allen, M., and Delitsky, M.: 1991, *Nature* **352**, 316-318

Johnson, R. L.: 1989, *Geophysical Res. Letters* **16**, 1233-1236

Keane, J. V.: 1997, 'Laboratory Simulation of Interstellar Ices Containing Cyanic Isomers', MS Thesis, Leiden University

Luu, J. X., Jewitt, D. C., and Trujillo, C.: 2000, *ApJ* **531**, L151-L154

Moore, M. H., Donn, B., Khanna, R. K., and A'Hearn, M. F.: 1983, *Icarus* **54**, 388-405

Moore, M. H., Ferrante, R. F., and Nuth, J. A., III: 1996, *Planetary and Space Science* **44**, 927-935

Moore, M. H. and Hudson R. L.: 1998, *Icarus* **135**, 518-527

Moore, M. H. and Hudson R. L.: 2000, *Icarus* **145**, 282-288

Moore, M. H. and Hudson, R. L.: 2003, *Icarus* **161**, 486-500

Moore, M. H. and Khanna, R. K.: 1991, *Spectrochim. Acta* **47A**, 255-262

Mumma, M. J., DiSanti, M. A., DelloRusso, N. Fomenkova, M. Magee-Sauer, K.,

Kaminski, C. D., and Xie, D. X.: 1996, *Science* **272**, 1310-1314

Noll, S. K., Luu, J. and Gilmore, D.: 2000, *ApJ* **119**, 970-976

Owen, T. C., Roush, T. L., Cruikshank, D. P., Elliot, J. L., Young, L. A. deBergh, C., Schmitt, B., Geballe, T. R., Brown, R. H., and Bartholomew, M. J.: 1993, *Science* **261**, 745-748

Palumbo, M. E., Castorina, A. C., and Strazzulla, G.: 1999, *Astron. Astrophys.* **342**, 551-5 62

Quirico, E., Doute, S., Schmitt, B., deBergh, C., Cruikshank, D. P., Owen, T. C., Geballe, T. R., Roush, T. L.: 1999, *Icarus* **139**, 159-178

Schutte, W. A., Allamandola, L. J. Sandford, S. A.: 1993, *Icarus* **104**, 118-137

Soderblom, L. A., Becker, L., Bennett, G., Boice, D. C., Britt, D. T., Brown, R. H., Buratti, B. J., Isbell, C., Giese, B., Hare, T., Hicks, M. D., Howington-Kraus, E., Kirk, R. L., Lee, M., Nelson, R. M., Oberst, J., Owen, T., Rayman, M. D., Sandel, B. R., Stern, S. A., Thomas, N., and Yelle, R. V.: 2002, *Science* **296**, 1087-1091

Table I. Detections of ices and other solid-phase materials

at the edge of the solar system

Object	Solid-Phase Detection	Energy Flux[a] eV cm^3 sec^{-1}	
		Cosmic Rays (MeV) H$^+$	UV Photons
Centaurs	H_2O, CH-containing ices (CH_3OH?), silicates, organics ("tholin")	~10^7	~3×10^9 - 1×10^{10}
Triton	N_2, CH_4, CO, CO_2, H_2O	~10^7	~3×10^9
Pluto	N_2, CH_4, CO (and H_2O?)	~10^7	~1×10^9
Charon	H_2O, NH_3, NH_3 hydrate	~10^7	~1×10^9
Edgeworth-Kuiper Belt Objects	H_2O, CH-containing ices (CH_3OH?), silicates	~10^7	~1×10^9
Comet Hale-Bopp[b]	H_2O	~10^7	~1×10^9
Comet Borrelly[b]	2.39-μm nuclear feature	~10^7	~1×10^9

[a]Estimates based on values for Pluto (Johnson, 1989) assuming a $1/r^2$ dependence for the UV photon flux, and a constant CR flux.

[b]Many coma molecules observed for this comet and most others.

Table II. Radiation products in ices at 10 - 20 K, along with products

detected after warming

Ice Mixture	Radiation Products at 10 – 20 K[a]	T (K) After Warming	Products Remaining[a]	Ice Environment
$H_2O + CH_4$ (10:1)	CO, CO_2, C_2H_6 $\underline{CH_3OH}$, C_2H_5OH	~100	$\underline{CH_3OH}$, C_2H_5OH (CH_4, CO_2, and CO)[b]	Comets, (KBOs, Centaurs?)
$H_2O + CO$ (10:1)	$\underline{H_2CO}$, $\underline{CH_3OH}$, $HCOOH$, CO_2, H_2CO_3 HCO radical, $HCOO^-$	~100	$\underline{H_2CO}$, $\underline{CH_3OH}$, $HCOOH$, $\underline{H_2CO_3}$ $HCOO^-$ (CO_2, CO)[b]	Comets (KBOs, Centaurs?)
$N_2 + CH_4$ (100:1)	HNC, HCN, CH_2N_2, NH_3, HN_3	~35 - 100	$\underline{NH_4}^+$, CN^-, N_3^-	Pluto, Triton (Comets, KBOs, Centaurs?)
$N_2 + CO$ (100:1)	CO_2, $\underline{C_3O_2}$, N_2O, NO, NO_2, O_3	~35 - 100	$\underline{C_3O_2}$	Pluto, Triton (Comets, KBOs, Centaurs?)
$N_2 + CH_4 +$ CO (100:1:1)	HNC, HCN, $\underline{HNCO}$, CH_2N_2, NH_3, HN_3, N_2O, CO_2	~35 - 100	$\underline{NH_4}^+$, CN^-, $\underline{OCN}^-$, N_3^-	Pluto, Triton (Comets, KBOs, Centaurs?)

[a]Underlined products are described in this paper because (i) they are less volatile species likely to accumulate on KBO surfaces containing these ices or (ii) they form less volatile species with additional processing.

[b]Species detected at 100 K trapped in H_2O-ice over time scales of hours.

Table III. Band positions and strengths[*]

Species	Position (μm)		Band Strength	Fig. No.	Ref
Carbon Suboxide C_3O_2	T < 20 K	(T = 250 K)	10^{-18} cm molec^{-1}		
	2.19	**(2.20)**	**0.02****		
	2.29	**(2.29)**	**0.03**		
	2.34		**0.001**		
	2.67	(2.66)	3.8, **2.0**		a
	2.76				
	3.00	(2.99)		2	
	3.29	(3.30)	6		a
	3.63	**(3.63)**	**0.06**		
	3.75	**(3.75)**	**0.09**		
	4.17		8		a
	4.55		130		a
	4.66				
	4.74				a
Carbonic Acid H_2CO_3		(T = 250 K)	10^{-18} cm molec^{-1}		
		(3.49)		3	
	3.81	(3.82)	160 (**155**)		b
Ammonium NH_4^+		(T = 250 K)	10^{-18} cm molec^{-1}		c
		(2.21)	**0.15**		
		(2.24)	**0.07**		
		(3.2)	**26**	4, 5	
		(3.3)	**37**		
		(3.5)			
Cyanate OCN^-	T < 20 K	(T = 250 K)	10^{-18} cm molec^{-1}		
	4.617	**(4.610)**	20	5	d
Polyoxymethylene POM $(H_2CO)_n$		(T ≥ 200 K)	10^{-20} cm^2 (C-atom)$^{-1}$		
		(2.24)	**0.6**		
		(3.36)	4.5	6	e
		(3.42)	6.0		e
		(3.58)	0.85		e
Ethylene Glycol $(CH_2OH)_2$	T < 20 K	(T = 100 K)	10^{-18} cm molec^{-1}		
	2.29	**(2.29)**	**0.1**		
	2.48	**(2.48)**	**0.25**	7	
	3.40	**(3.40)**			
	3.48	**(3.48)**			

[*]Data in parentheses were recorded at the higher temperatures. Data in bold are new values whereas data not in bold are from the literature as referenced. **Values based on $A = 6$ x 10^{-18} cm molec^{-1} for 3.29 μm band.

(a) Gerakines and Moore (2001)

(b) Gerakines *et al.* (2000)

(c) Average value for 6.96 μm band is 30 x 10^{-18} cm molec^{-1} based on: d'Hendecourt and Allamandola (1986); Grim and Greenberg (1987); Demyk *et al.* (1998); R. K. Khanna (2003, private communication)

(d) Average based on: Grim *et al.* (1989); Demyk *et al.* (1998); Keane (1997); R. K. Khanna (2003, private communication)

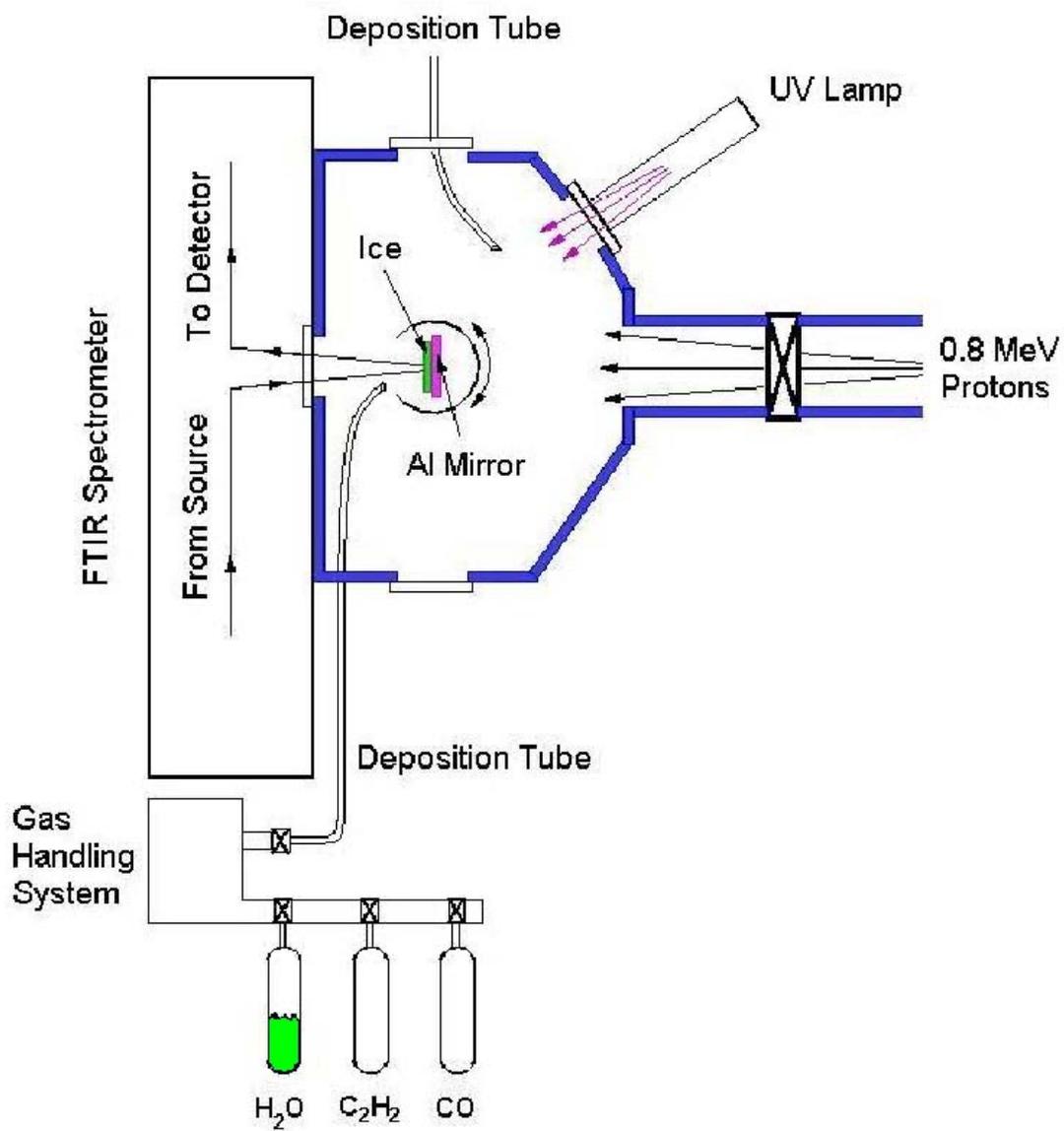(e) Schutte *et al.* (1993)

Figure 1. Schematic of laboratory set-up.

Figure 2. Spectrum of carbon suboxide (C_3O_2) from 1 - 5 μm at T < 20 K. The region from 1 - 4 μm is shown vertically expanded by a factor of ~7. Additional expansion around 2.2 μm (upper left) reveals several weak overtone bands. For comparison, the lower truncated spectrum shows pure CO ice at T < 20 K. (The 2.70-μm feature is H_2O contamination.)
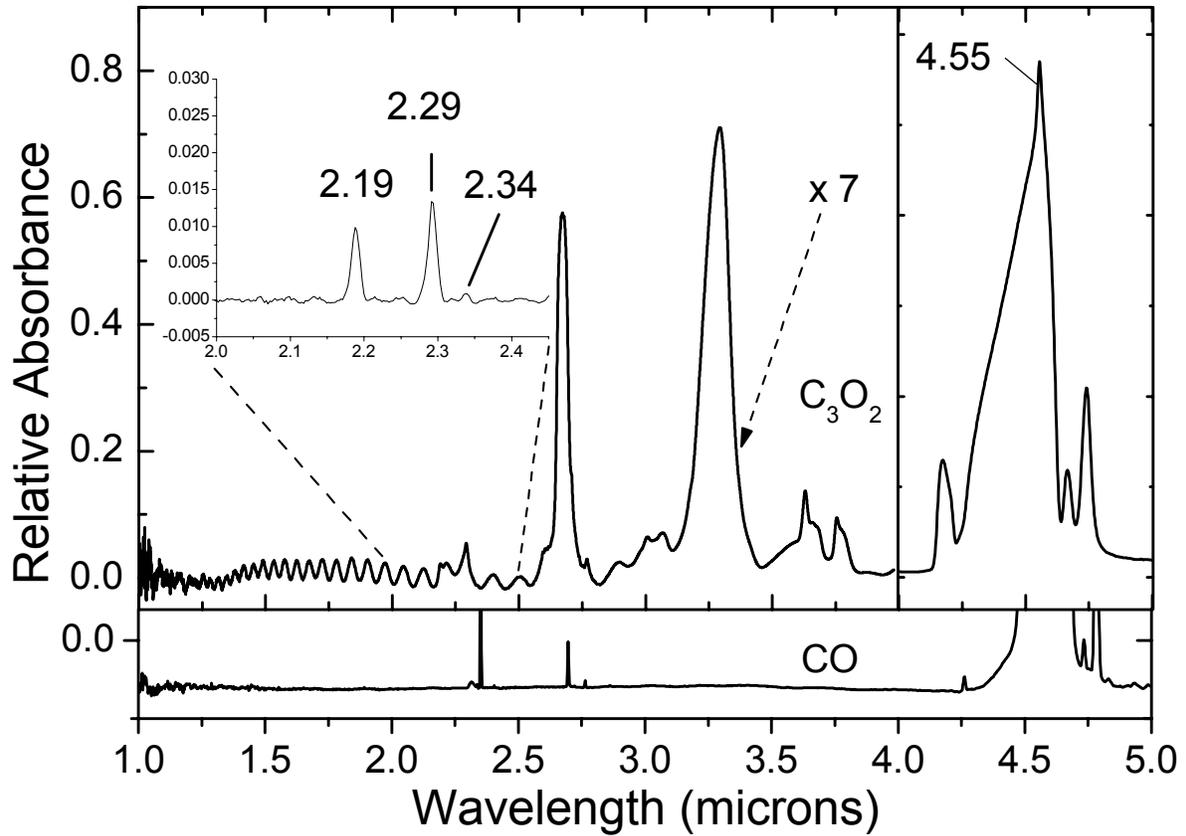
Figure 3. Spectrum of carbonic acid (H_2CO_3) at 250 K. This molecule is a dominant product after ion irradiation of icy $H_2O + CO_2$, and is less volatile than H_2O. For comparison, the spectrum of unirradiated $H_2O + CO_2$ is shown (truncated) at the bottom.
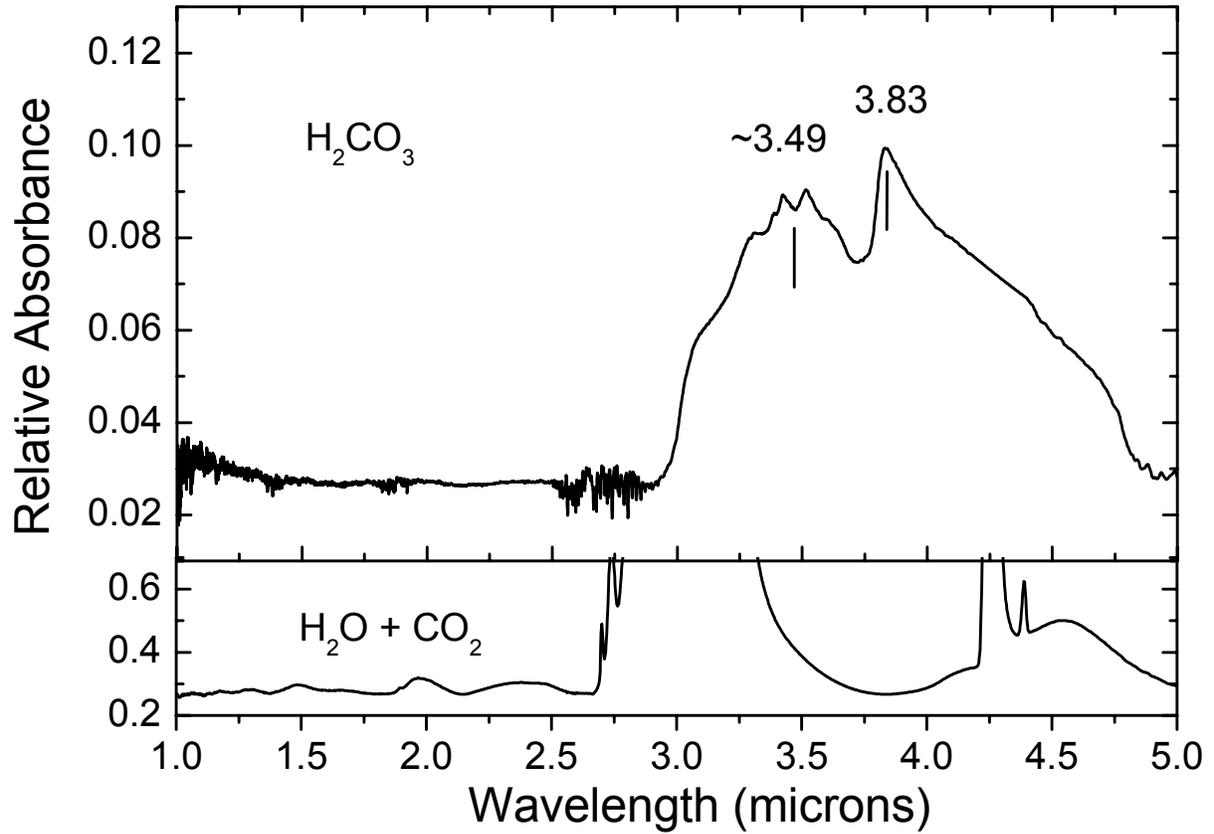
Figure 4. Spectrum of ammonium chloride (NH_4Cl) at 250 K. For comparison, the spectrum of pure NH_3 at 120 K is shown, and the position of the fundamental vibration of HCl is indicated with an arrow at 3.6 μm. Weaker overtone bands of NH_4^+ are evident in the expanded view (uppermost trace) and can be compared to those of NH_3 (lower).
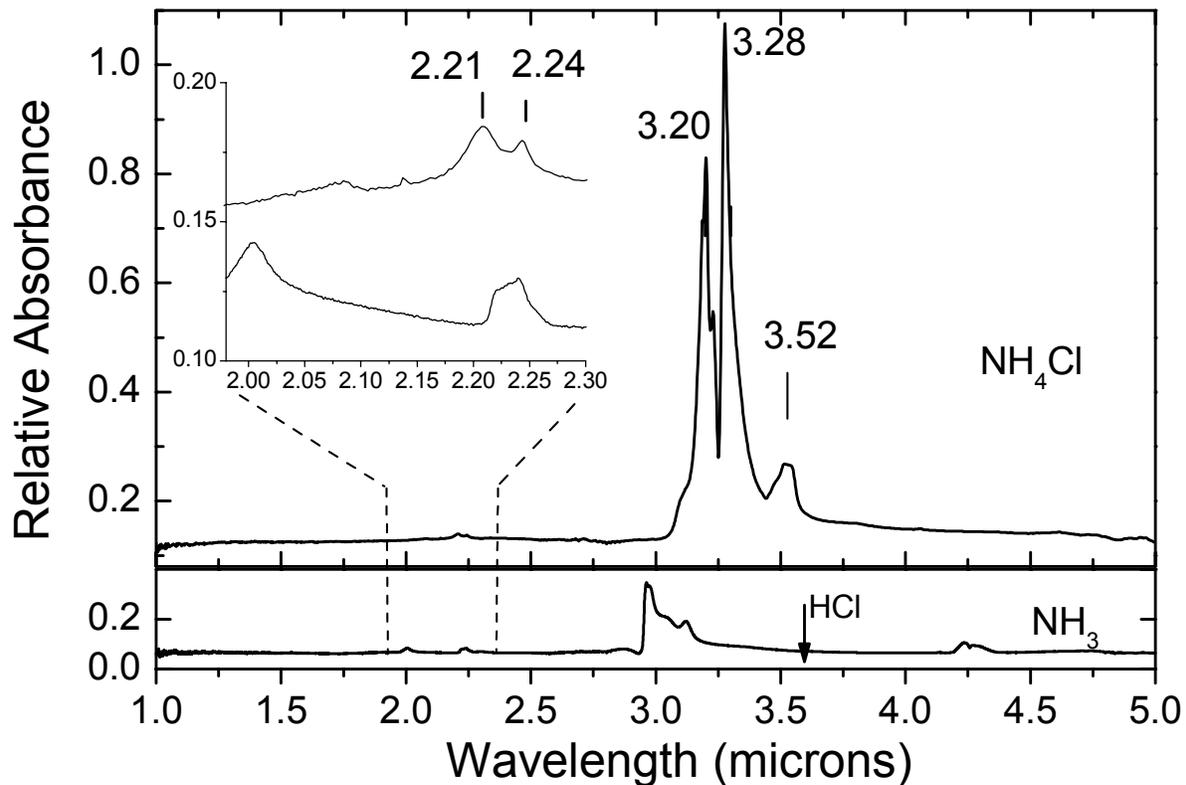
Figure 5. Spectrum of ammonium cyanate (NH₄OCN) at 250 K. For comparison, the spectrum of pure HNCO at 10 K is shown. (The spectrum of pure NH₃ is in Figure 4.)
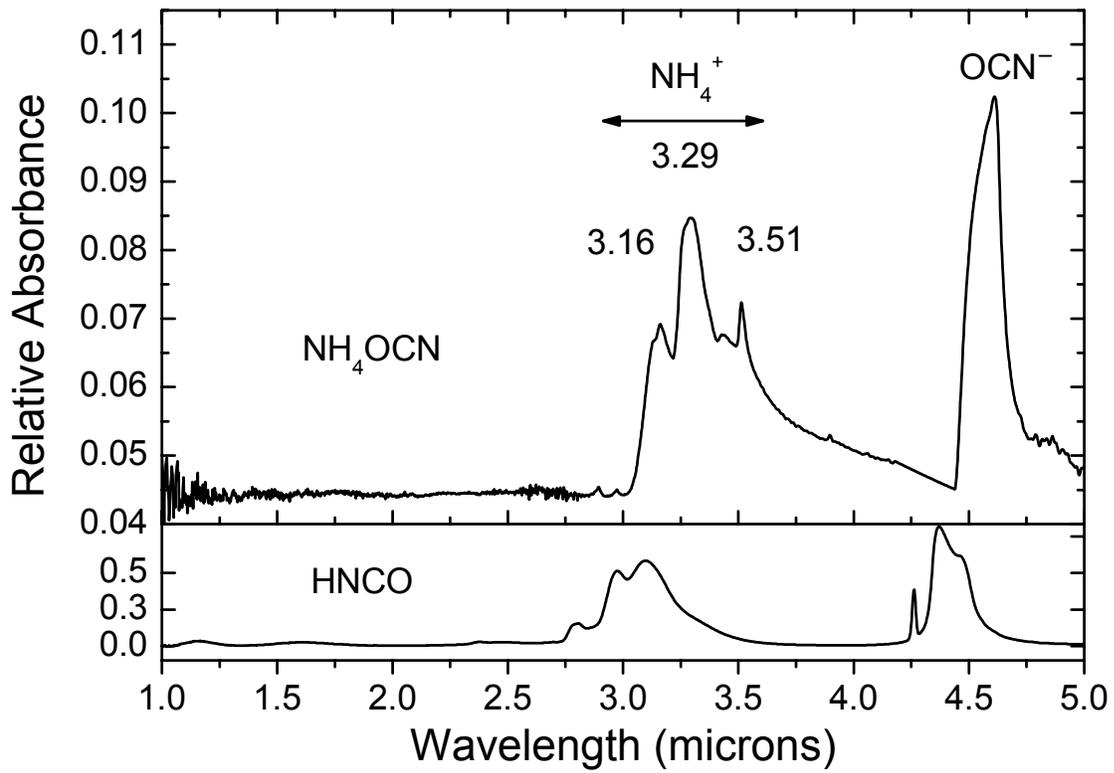
Figure 6. Spectrum of polyoxymethylene (POM or (H₂CO)ₙ), at 200 K. Slow warming of an H_2CO + NH_3 (50:1) ice condensed at T < 20 K resulted in the formation of this polymer. For comparison, the spectrum of pure H_2CO below 20 K is shown. (The spectrum of pure NH_3 is in Figure 4.) Weak overtone bands of POM are evident in the expansion at the upper left.
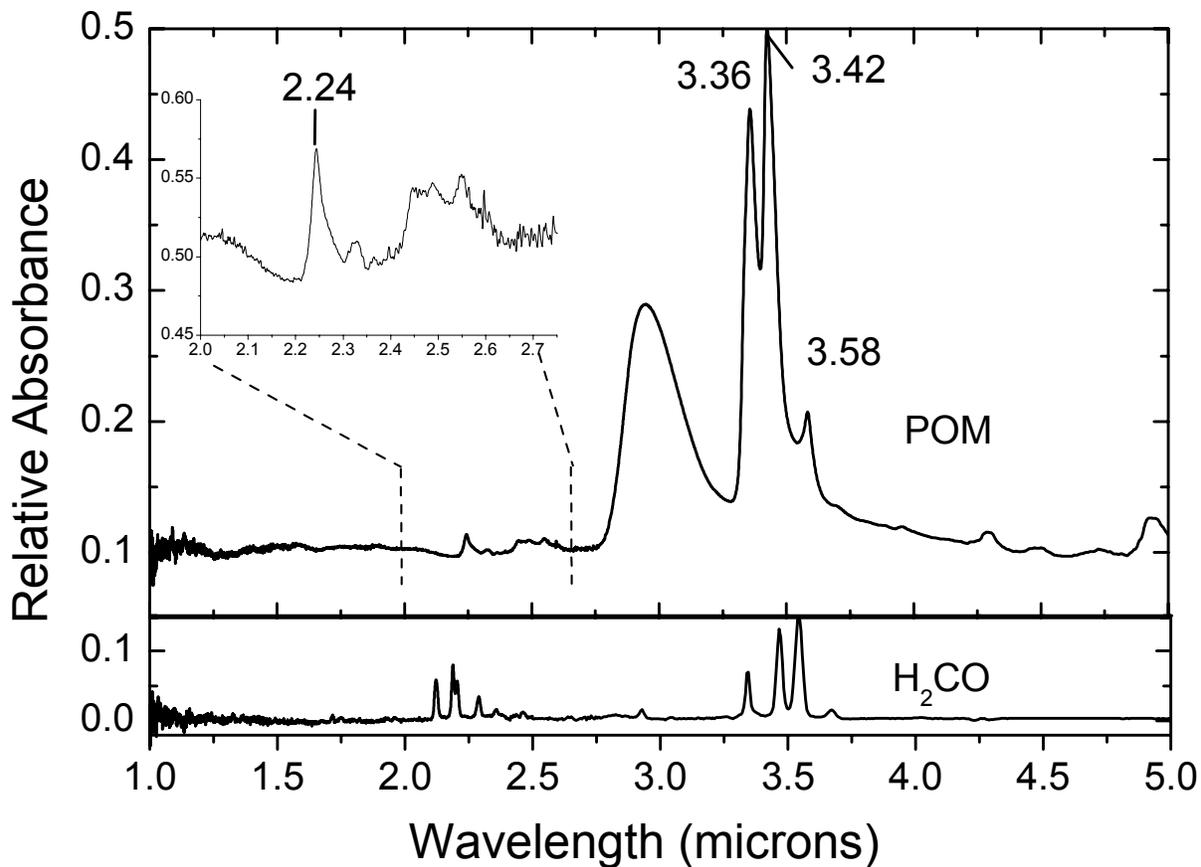
Figure 7. Spectra of ethylene glycol ((CH₂OH)₂) and CH₃OH, both samples at T < 20 K. Expansion of the 2.5-μm region reveals weak overtone bands of both $(CH_2OH)_2$ and CH_3OH.